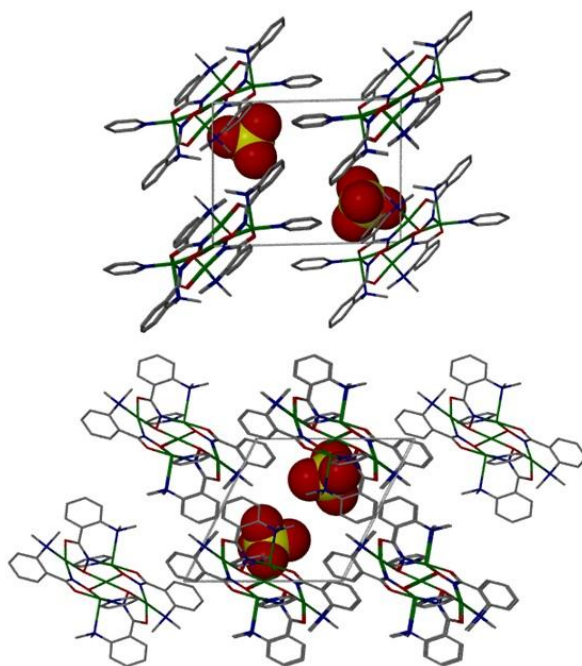


*Electronic Supplementary Information*

**Progressive Decoration of Pentanuclear Cu(II) 12-Metallacrown-4 Nodes Towards Targeted 1- and 2D Extended Networks**

*Cecelia McDonald,<sup>a</sup> Teresa Whyte,<sup>a</sup> Stephanie M. Taylor,<sup>c</sup> Sergio Sanz,<sup>c</sup> Euan. K. Brechin,<sup>c</sup>  
Declan Gaynor<sup>b\*</sup> and Leigh F. Jones<sup>a\*</sup>*



**Fig. S1** Packing arrangement observed in **2** as viewed along the *b* (top) and *a* (bottom) cell directions. The pyridine solvent of crystallisation has been omitted for clarity. ClO<sub>4</sub><sup>−</sup> counter anions are space-fill represented.

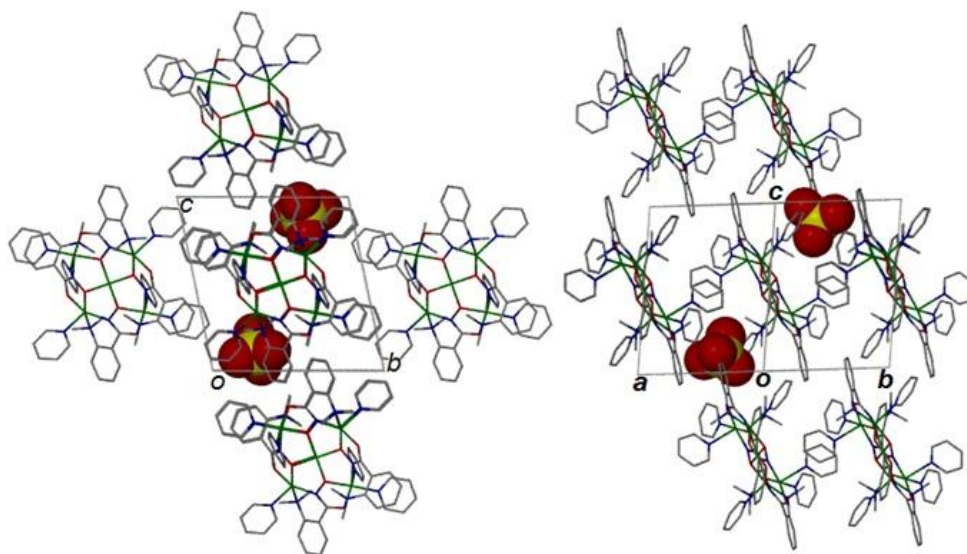


**Figure S2** Packing observed in **3** as viewed along the *a* axis (left) and along the *ab* direction of the unit cell (right) . All Hydrogen atoms have been omitted for clarity. The  $\text{ClO}_4^-$  counter ions within the cell are represented as space-fill.

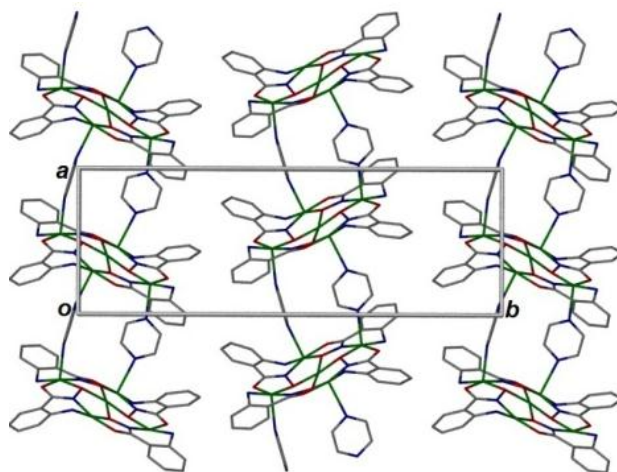


**Figure S3** Three 1-D rows in **6** illustrating the alternating  $[\text{Cu}_5]$  tilt angles along the *b* direction of the unit cell.

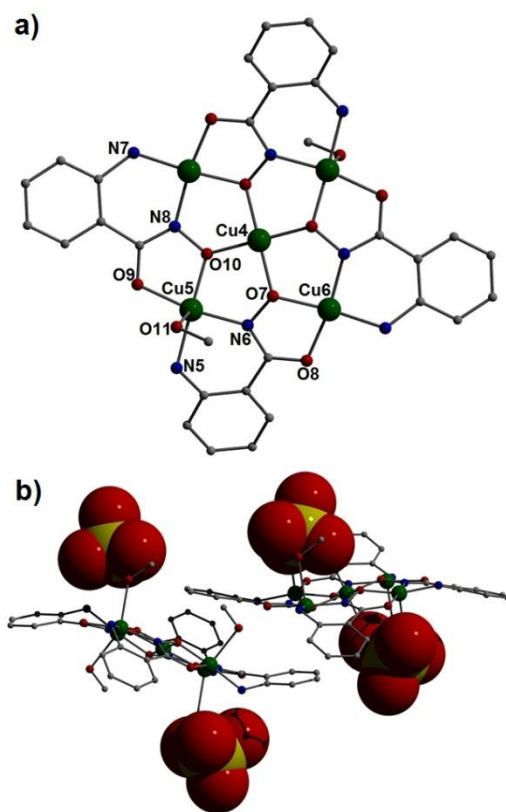


**Figure S4** (a) Crystal structure of **7** showing only one of the two [Cu<sub>5</sub>] moieties in the asymmetric unit. (b) The asymmetric units in **7** illustrating the close proximity of the two crystallographically unique [Cu<sub>5</sub>] species. The ClO<sub>4</sub><sup>-</sup> counter anions are represented as space-fill.

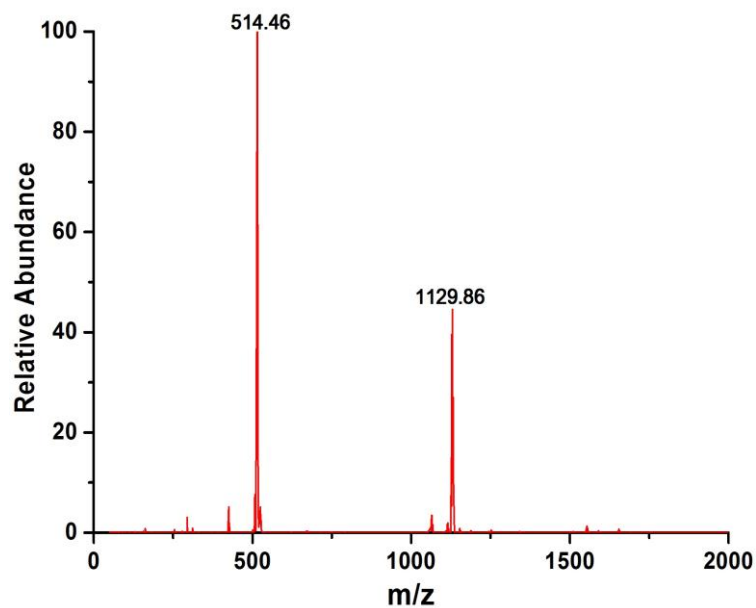


**Fig. S5** Mass spectrum of **1** from a 50:50 MeCN/H<sub>2</sub>O solvent matrix. TOF MS-ES (%) m/z:  
514.46 (100, [Cu(II)<sub>5</sub>(L<sub>1</sub>)<sub>4</sub>]<sup>2+</sup>), 1129.86 (44, [{Cu(II)<sub>5</sub>(L<sub>1</sub>)<sub>4</sub>} + {ClO<sub>4</sub>}]<sup>+</sup>).

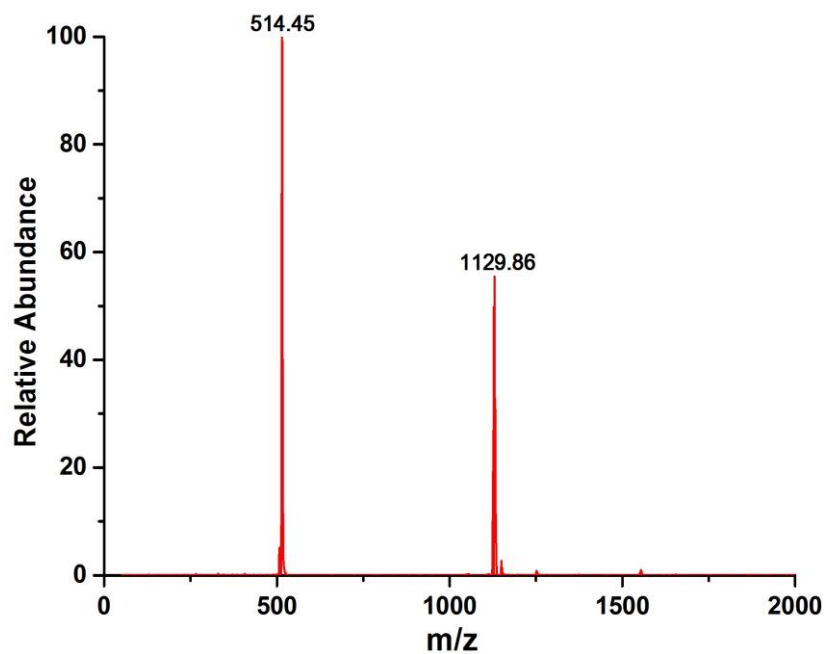


**Fig. S6** Mass spectrum of **2** from a 50:50 MeCN/H<sub>2</sub>O solvent matrix. TOF MS-ES (%) m/z:  
514.45 (60, [Cu(II)<sub>5</sub>(L<sub>1</sub>)<sub>4</sub>]<sup>2+</sup>), 1129.86 (55, [{Cu(II)<sub>5</sub>(L<sub>1</sub>)<sub>4</sub>} + {ClO<sub>4</sub>}]<sup>+</sup>).

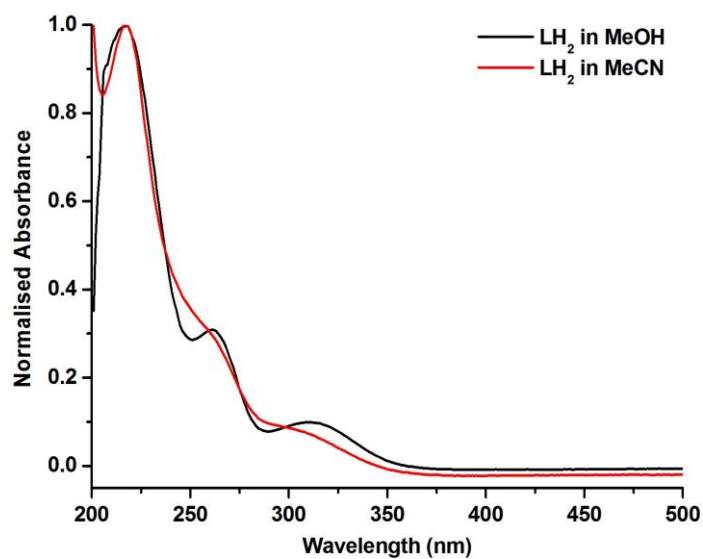


**Fig. S7** Overlay UV-vis spectra of  $L_1H_2$  obtained from MeOH (black line) and MeCN (red line) solutions.

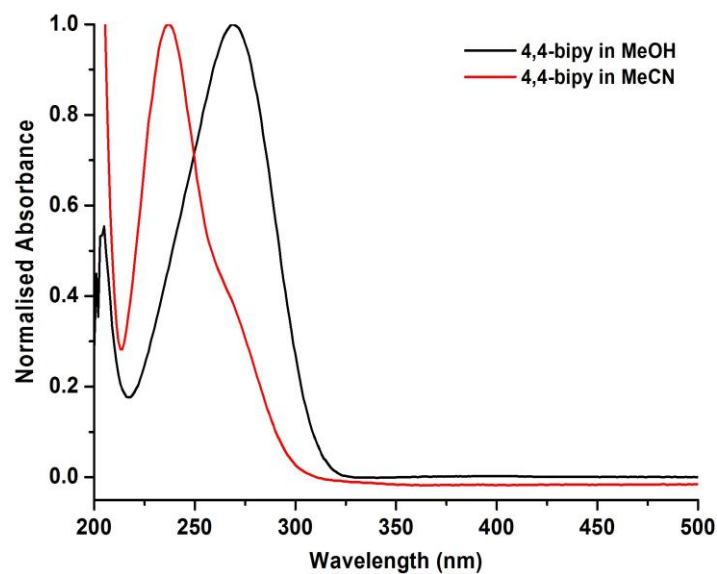


**Fig. S8** Overlay UV-vis spectra of the 4,4'-bipyridine ligand obtained from MeOH (black line) and MeCN (red line) solutions.

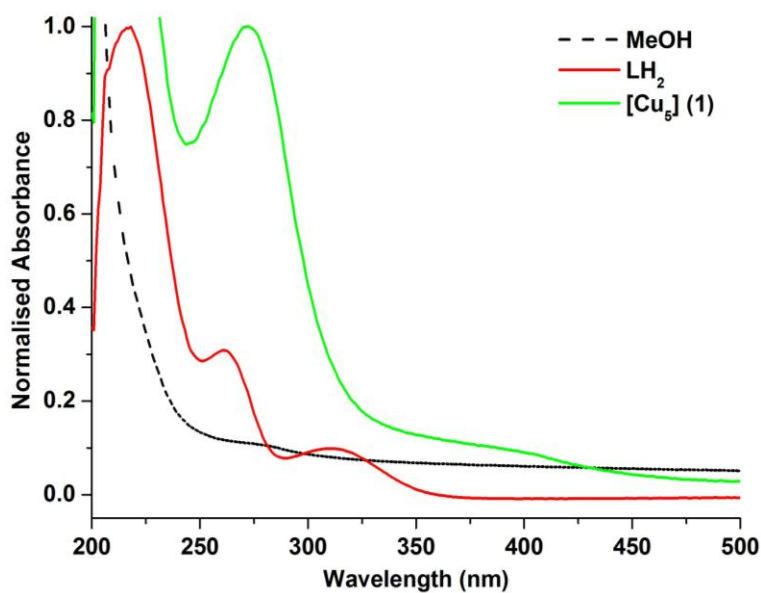


**Fig. S9** Overlay UV-vis spectra of MeOH (dashed black line),  $L_1H_2$  (red line) and  $[Cu(II)_5(L_1)_4(MeOH)_2](ClO_4)_2$  (**1**) (green line).

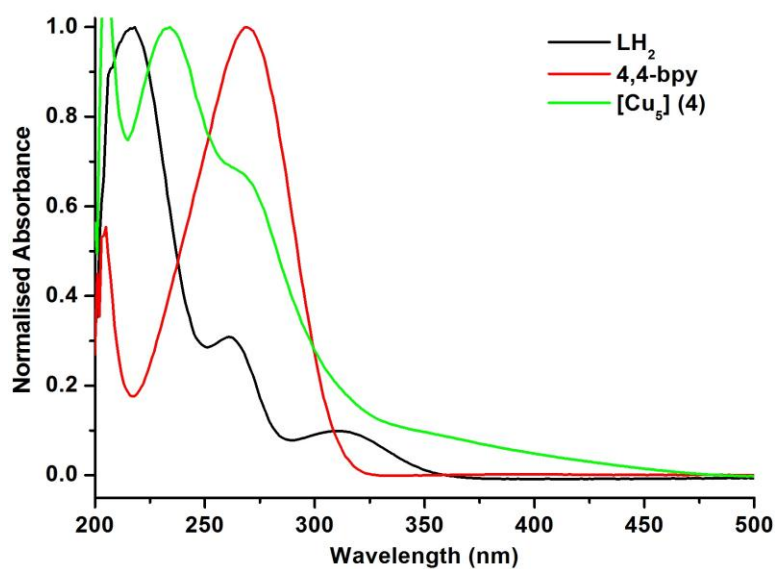


**Fig. S10** Overlay UV-vis spectra in MeOH of  $LH_2$  (black line), 4,4'-bipyridine (red line) and  $\{[Cu_5(L_1)_4(4,4'\text{-bipy})_3](ClO_4)_2(H_2O)}_n (4)$  (green line).

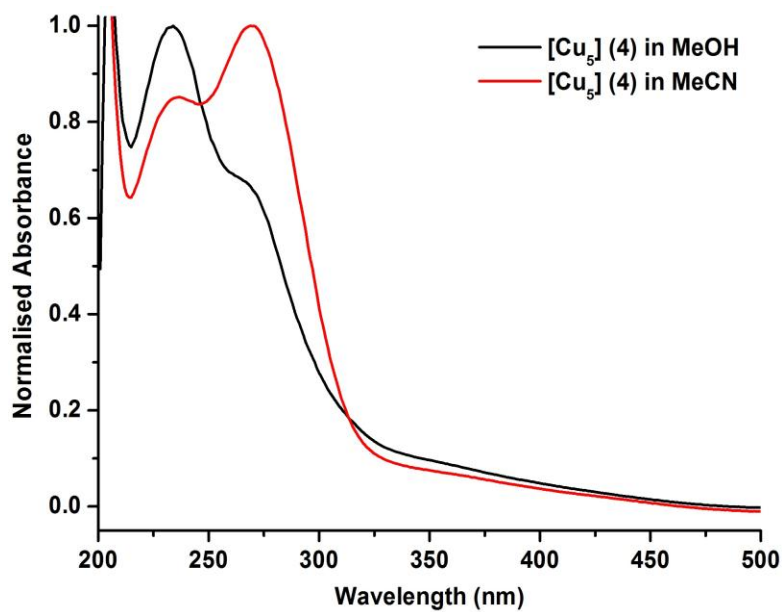


**Fig. S11** Overlay UV-vis spectra of  $\{[Cu_5(L_1)_4(4,4'\text{-bipy})_3](ClO_4)_2(H_2O)}_n (4)$  obtained from MeOH (black line) and MeCN (red line) solutions.

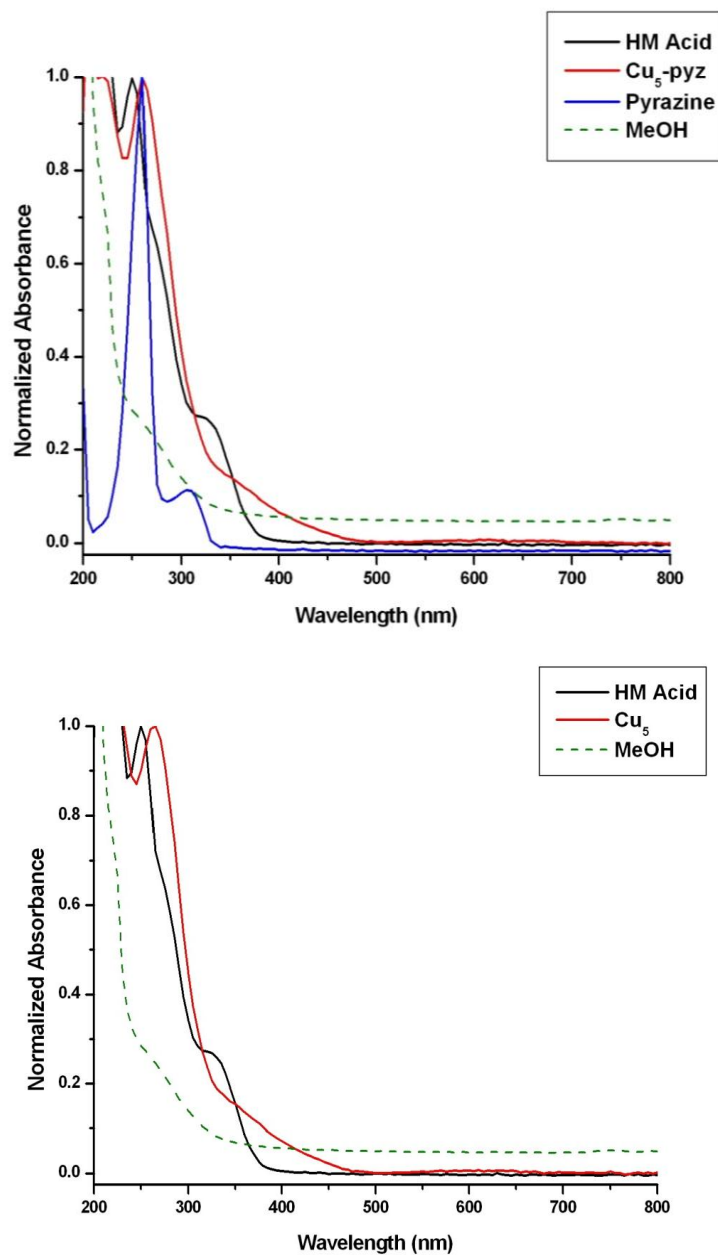


**Fig. S12** (top) Overlay UV-vis spectra in MeOH (dashed line) of  $L_2H_2$  (black line), pyrazine (blue line) and  $\{[Cu_5(L_2)_4(pz)_2(MeOH)_3](ClO_4)_2 \cdot MeOH\}_n$  (**6**) (red line). (Bottom) Overlay UV-vis spectra in MeOH (dashed line) of  $L_2H_2$  (black line) and  $[Cu_5(L_2)_4(MeOH)_4](ClO_4)_2 \cdot H_2O$  (**7**) (red line).



**Fig. S13** The UV-vis methanolic solutions of  $L_1H_2$  (left),  $[Cu(II)_5(L)_4(MeOH)_4(ClO_4)_2]$  (**1**) (middle) and the extended network (*dissociated in solution*)  $\{[Cu(II)_5(L)_4(4,4-bipy)_3](ClO_4)_2(H_2O)\}_n$  (**4**) (right) used in this work.